Pattern flattening for orthotropic materials

J. McCartney*, B.K. Hinds, K.W. Chong

*School of Mechanical and Manufacturing Engineering, The Queen's University of Belfast, Ashby Building,
Stranmills Road, BT9 5AH Belfast, Northern Ireland, UK*

Abstract

In many applications it is necessary to define good-fitting 2D flattened patterns for user-defined regions of a larger 3D surface. This paper describes the major stages involved in pattern flattening and illustrates the process with examples. In generating 2D patterns, some distortion is inevitably involved if the target 3D surface is not developable. For situations where distortion is required, it can be quantified in terms of the energy that must be imparted to the 2D flattening in localised areas so that it takes-up the original 3D region of the surface. An orthotropic strain model is adopted to convert the strain values to energy values. Starting with a bi-parametric definition of a large 3D surface, an arbitrary defined region is specified by the user in terms of a contiguous series of cubic curves lying on the bi-parametric plane. To extract the 3D region, a polygon list is generated to represent the surface. The triangulation process is based on a 'marching front' algorithm. A process is described which then flattens this polygon list and performs an energy minimisation analysis every time the process attempts to flatten an over-constrained triangle. Further consideration is made of seam insertion in the 3D surface definition and of adaptively modifying the triangulation process so that more triangles are used in areas of high-energy concentration. Examples are also presented to illustrate the sensitivity of the strain profiles to the fabric grain direction when the pattern is applied to the 3D surface.
© 2004 Published by Elsevier Ltd.

1. Introduction

In many industries, three-dimensional (3D) products or components are manufactured from raw material that is initially supplied in two-dimensional (2D) form. Such industries include garment manufacture, sail making and ship hull production. Since the 3D surfaces that are ultimately assumed by the raw material are not usually developable surfaces [1], inevitably there has to be some distortion of the material involved in progressing from the raw 2D state to the final 3D form. However, it is important to realise that the design process usually proceeds in the reverse direction to the manufacturing process, i.e. the starting point is generally the target 3D shape with the 2D pattern being the variable that has to be determined by adopting some particular criterion. This paper addresses this situation by adopting an energy model to simulate the process of creating a 2D form to take-up the target 3D shape. The model assumes an orthotropic material, which is used where the elastic performance is sensitive to the grain direction with respect to two orthogonal axes (warp and weft). In doing so, it provides an objective indication of how good a particular 2D pattern is and it also quantifies the energy reductions resulting from applying mechanisms such as darts and gussets to improve the fit performance. The actual surface representation used to represent the target 3D form is a polygon list. The quality of this underlying mesh is critical to the success of the flattening process. The paper also outlines how mesh triangulations are generated that are sympathetic to the 3D target shape and the particular seam configuration applied.

2. Previous work

There has been considerable interest for many years in obtaining patterns to cover 3D shapes. In an early paper,

---

* Corresponding author. Tel.: +44 2890 274127; fax: +44 2890 661729.
  E-mail address: j.mccartney@queens-belfast.ac.uk (J. McCartney).

Manning [2] proposed a method of obtaining a pattern for a 3D surface. Firstly, an isometric tree was defined on the 3D surface. For the discrete 3D curves defined by the spine and branches of the tree, a pattern was obtained by plotting their geodesic curvature versus arc length on a plane whilst preserving the angles at nodes. Hinds et al. [3] developed this approach further and obtained patterns for a 3D surface by first covering the surface with quadrilateral platelets and rolling out each strip of platelets in turn, starting from a spine. Similar methods were examined by Azariades and Asparagathos [4]. They first searched for the best generating line on the 3D surface from which to initiate the development process. There was then a piecewise development onto the 2D plane of these strips followed by a final stage to reduce the gaps and overlaps between the strips. Kim and Kang [5] used a similar method for garment pattern generation but allowed some shear in the strips being rolled out in order to coalesce several small darts into a simple large dart that would be more acceptable in tailoring practice.

A related problem occurs in texture rendering for computer images where it is important to reduce mapping distortions. Shaffer and De Starler [6] first used a technique called angle based flattening that minimised the angular distortion of the mapping. This was followed by a further procedure that reduced length distortions in the mapping. They raised the issue of the trade-off between angular and linear distortions.

Whereas texture rendering is concerned with the geometric distortions in the mapping, in pattern development it is appropriate to relate geometric distortion to strain energy in the material being used and several authors have followed this approach. Azariadis et al. [7] linked the in-plane bending of strips in the development plane to an energy function. Optimisation methods were employed to find minimum energy patterns.

McCartney et al. [8] and Wang et al. [9] modelled 3D surfaces with triangular facets. The flattening process required length changes to triangle edges that were combined in an energy function. The best patterns were those associated with minimum energy. McCartney et al. also considered the insertion of darts or seam lines, the introduction of which releases strain energy in the flattening.

The development of 3D triangular meshes is associated with tensile distortion of individual edges whereas the main distortion energy in real fabrics is associated with stretch and shear of the fabric weave. Ohsaki and Fujiwara [10] used FE methods to model fabric structures in architectural applications. In these instances, the 3D fabric structure is required to be pre-stressed to maintain stability and stiffness against external loads. Also the curved 3D shape has to be formed from plane sheets by stretching the boundary of the sheet. Properties of the fabric sheet are included in the analysis with orthotropic elastic moduli, shear modulus and Poisson's ratio specified. The objective of this work was to achieve the target stresses in the 3D shape by connecting and stretching plane sheets.

The present work similarly takes account of the weave structure of the fabric with strain energy based on tensile and shear distortions. Unlike methods that assume isotropic fabric properties, it is shown that pattern distortion energy is sensitive to the fabric grain direction. This information is useful if it is necessary to limit one of the strains or if a seam is being introduced to reduce the deformation energy. Although not presently implemented, the process can incorporate defined non-linear fabric properties. The flattening process described here is made more robust by incorporation of a triangulation based on marching front methods. When seams are added, the seam edges are incorporated into the boundary description and the triangulation process is reworked. Also triangle intensification is applied in areas of high curvature.

3. Initial panel design and representation

The starting point for the process is the specification of the target 3D surface to be ultimately assumed by the material involved. The authors have developed a 3D design system [11] that is able to generate offset surfaces to underlying B-Spline surfaces derived from digitised body data. Typical underlying body surfaces can be the upper body torso in the case of garments or last forms in the case of shoe design. A 3D cursor enables a panel boundary area to be defined. Interior points are then supplied by offsetting appropriate underlying body surface points. This arrangement also enables final validation by offering a 3D template by which any pattern assembly can be assessed in terms of fit. However, this starting point does not detract from the overall applicability of the process described below since it is based on a polygon list representation that can be generated from virtually any 3D CAD system. Fig. 1 illustrates an initial description of a garment panel. Interior points have been supplied by identifying underlying body digitised points that are enclosed by the panel boundary for a given density of intensification in each of the parametric directions, i and j. Delaunay triangulation has then been performed (on the parametric plane) on the complete set of points—boundary points and interior points, in order to generate a polygon list. This process has been described elsewhere [12]. Whenever this polygon list was subjected to further analysis it was discovered that the quality of the mesh in terms of variation in triangle geometry was not conducive to good results and flattening algorithm performance. The use of interior points aligned with parameters of the underlying body was not desirable at times because it can produce an unacceptable variation in spacing in 3D space even though the spacing in parameter space was uniform. The authors have developed a marching front type algorithm [13] that generates interior points by repetitively shrinking the outer boundary while maintaining a constant
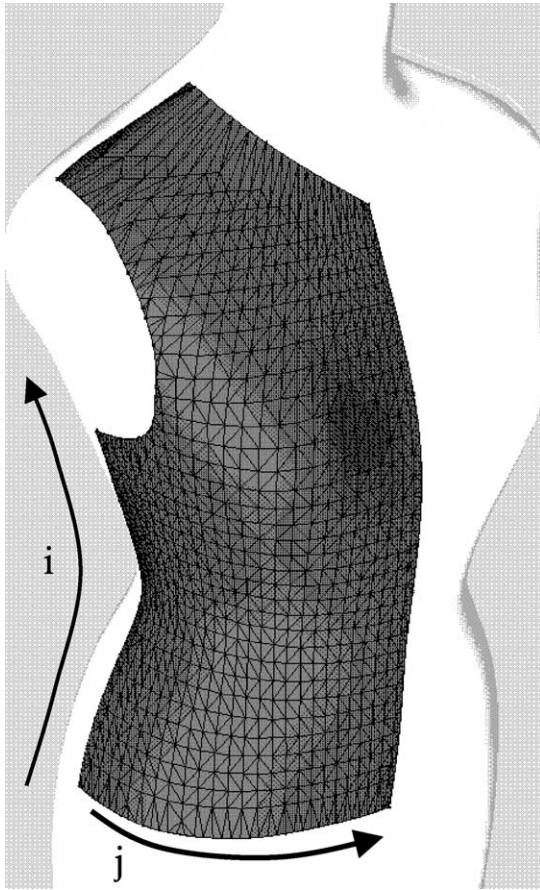
Fig. 1. Initial garment panel triangulation.

offset with respect to the underlying body. This method of triangulation can be controlled by nominating a specific spacing value in 3D space for points on interior fronts and the distance between fronts. Fig. 2 illustrates the progression of the triangulating algorithm to the same boundary used for the panel in Fig. 1. Not only does this method generate a more uniform triangulation, it also produces a triangulation that is more sympathetic to the flattening process that is described later. The experience of the authors in developing and using flattening algorithms is such that they consider it vital that a good triangulation of the 3D surface to be flattened is used. If coarse or misaligned triangulations are adopted then this can lead to excessive strains being concentrated within a single triangular representation. Under extreme circumstances, individual triangles produce a 2D representation that have been flipped and so generate a corrupt flattened pattern.

As with many algorithms that operate on a polygonal form of a continuous surface, there is a trade-off between accuracy in representing the continuous surface and the processing time and memory requirements involved in performing the algorithm. However, if it is decided to use a specific number of polygons, then there are various ways in which the same number of polygons can be generated from the same continuous surface. Each will exhibit different levels of accuracy in representing the continuous surface. For the purposes of this work, the error is defined as the difference between the actual offset at the centre of area of the triangle and the constant offset existing at all triangle vertices (Fig. 3(a)). Experience has shown that an equal sized mesh is often not the best arrangement for a polygon mesh. This is because there may be high variability of curvature displayed by the underlying body form. This results in variable errors being produced for each triangle in representing the theoretical continuous offset 3D surface. The approach adopted here is to initiate the moving front triangulation process (described above) by specifying a target size for the triangles. This will generate a set of triangles with a distribution of error values. An error threshold is then defined, above which indicates unacceptable error. For such cases, an intensification of the triangulation is effected in the neighbourhood of the triangle with the unacceptable error (Fig. 3(b) and (c)). As can be seen, the subdivision process guarantees that the previous centre of area which produced the unacceptable error (Fig. 3(b)) will be used as approximately the centre of area of a new smaller triangle and so result in a smaller error. The new subdivided triangles will each have their own new error values that should be significantly less than the previous unacceptable error. When applied to the panel representation in Fig. 2 and adopting an error threshold value of 0.3 mm, the triangulation of Fig. 4 results. As can be seen, this will obviously result in greater polygon intensification in the bust area where potentially problems can result in the flattening process if coarser densities are used.

4. Seam insertion

Darts and gussets are practical tools for introducing better interior fitting for 2D patterns. At the outset, darts and gussets are specified in a similar fashion. The location of a dart or gusset is determined by the designer who indicates a seam line that is initiated from a panel boundary and proceeds into the interior of the 3D surface. Note that for the flattening process described here, the seam location in 3D and its geometry in the interior of the panel are completely arbitrary and are not constrained to align with the original surface parameterisation.

Where the underlying surface is predominantly elliptical, the two sides of the seam splay apart—indicating that a dart should be inserted (Fig. 5). When this occurs, the two sides of the seam must be subsequently joined on the 2D pattern to implement the dart. Where the underlying surface is predominantly hyperbolic, the two sides of the seam will overlap—indicating that a gusset should be inserted (Fig. 6). When this occurs, the area of overlap provides an indication of the gusset geometry. An extra piece of material is then inserted between the two sides of the seam to implement the gusset. It is possible to have a combination of both dart and gusset along the same seam.
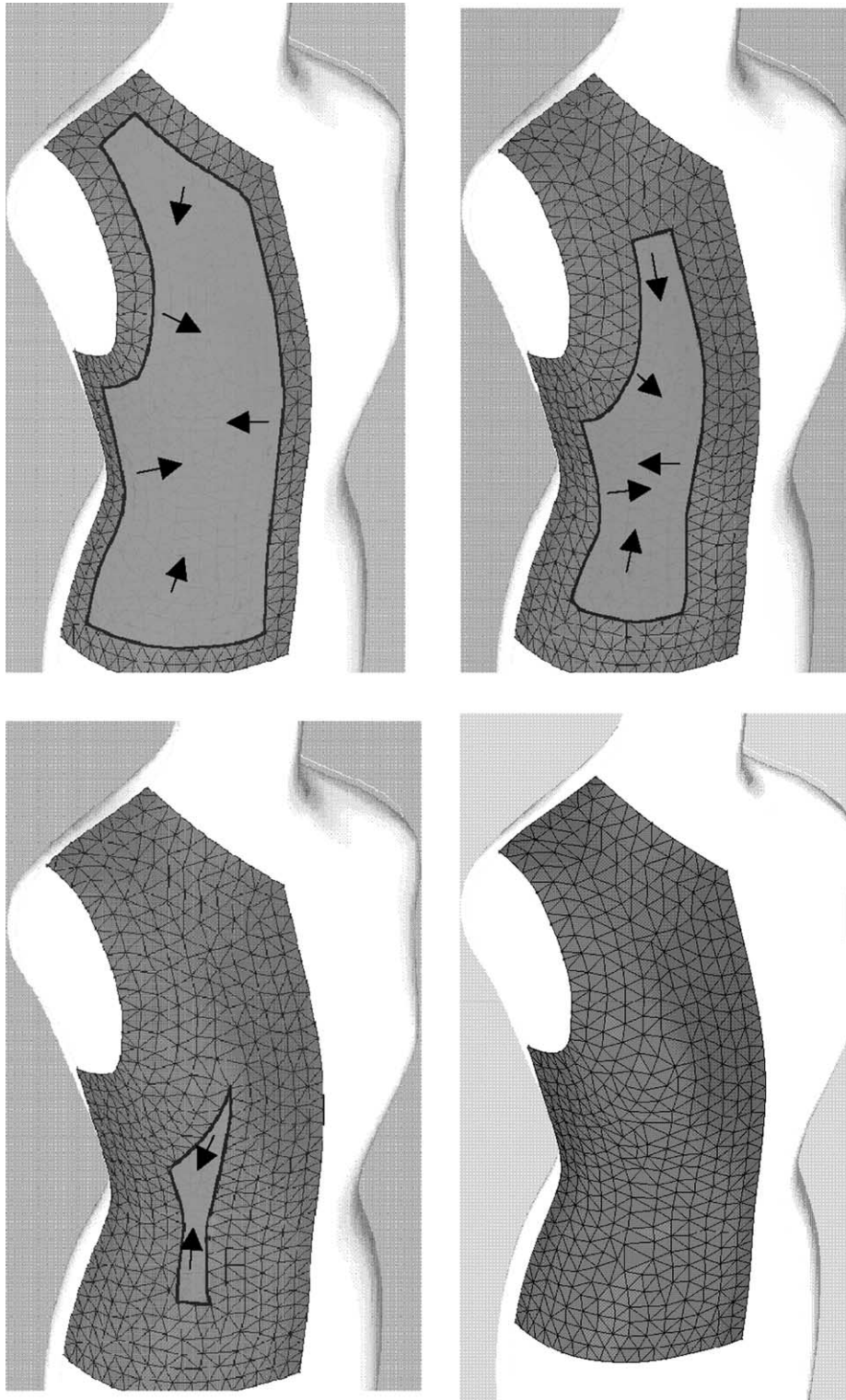
Fig. 2. Progression of marching front triangulation.

Once a seam line has been specified in this way it will influence the triangulation process described above. This places an additional constraint on the triangulation process s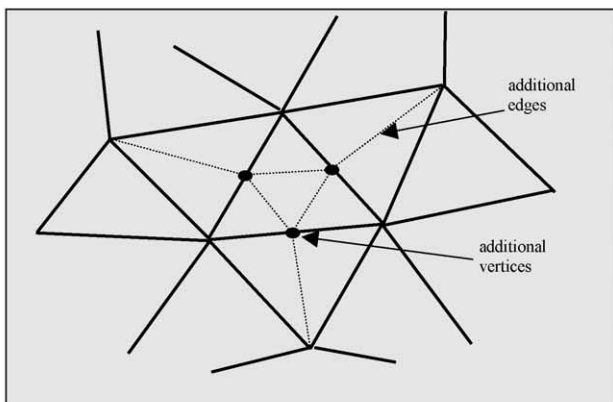ince the dart line must be represented by a series of edges and nodes. A re-triangulation process then maintains the seam representation. Such an effect is depicted in Fig. 7. In addition, the nodes and edges along the dart, except the innermost node, have one further feature. Although being
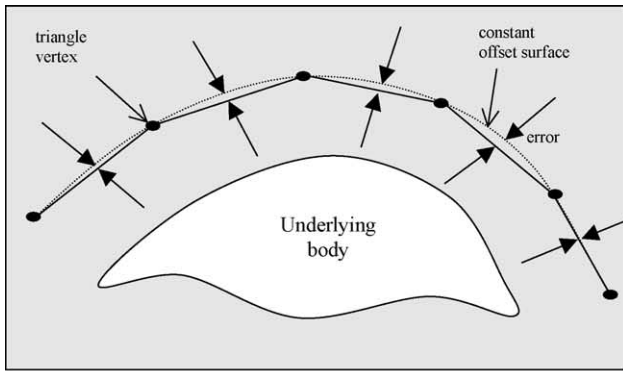
(a) offset error calculation
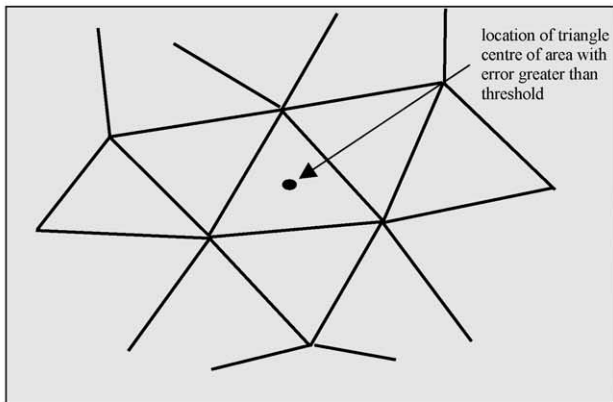
(b) before triangle subdivision

(c) after triangle subdivision

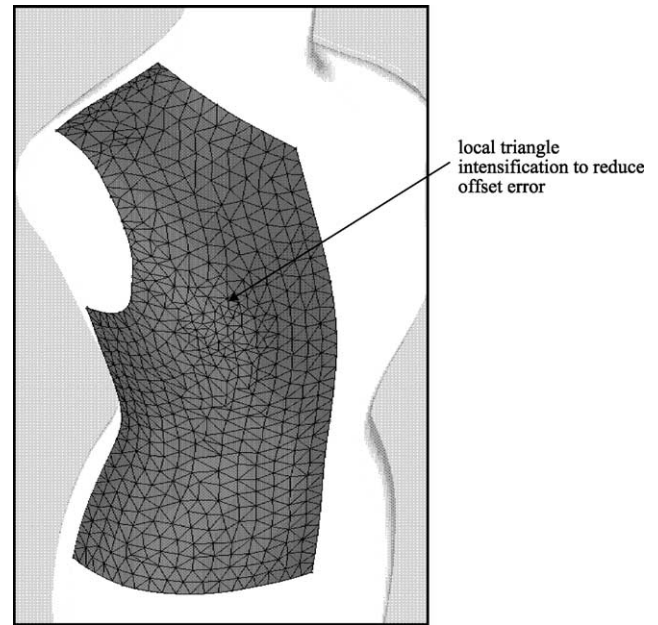Fig. 3. Triangular mesh intensification.

Fig. 4. Triangulation after intensification.

considered as fixed and it is the 2D geometry of each triangle that is regarded as variable during the flattening process. However, the fabric area covered by each 2D triangle in the flattening process is undistorted—it is the 3D triangle that will embody any distortion necessary.
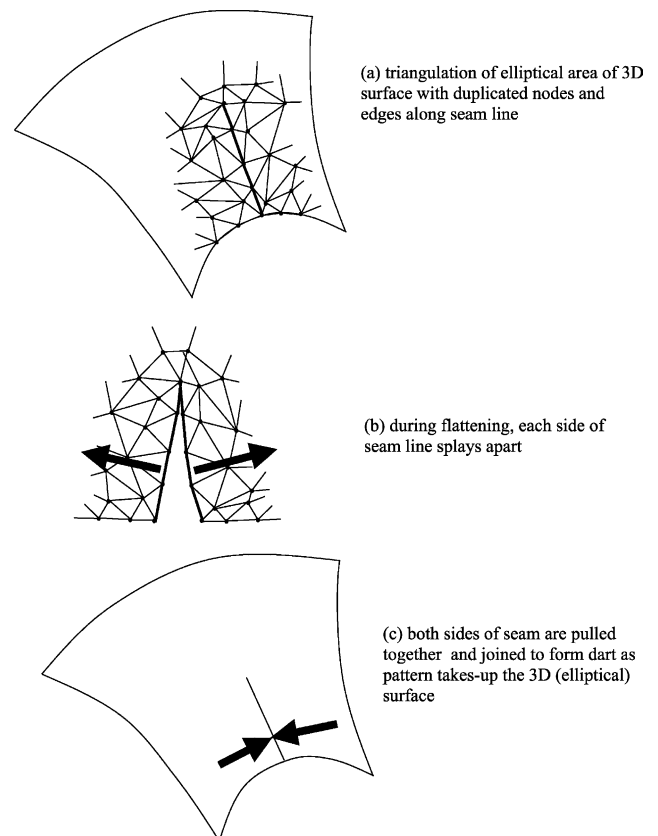

(a) triangulation of elliptical area of 3D surface with duplicated nodes and edges along seam line

(b) during flattening, each side of seam line splays apart

(c) both sides of seam are pulled together and joined to form dart as pattern takes-up the 3D (elliptical) surface

Fig. 5. Dart formation in 2D pattern.

viewed in 3D as an intact seam, the seam line nodes and edges are in fact duplicated for 2D flattening. Thus, during the flattening process, each side of the seam line has its own representation. This can lead to different configurations during the flattening process.

5. Energy model for fabric distortion

During the flattening process, a single triangle at a time is treated for flattening. The 3D geometry of each triangle is
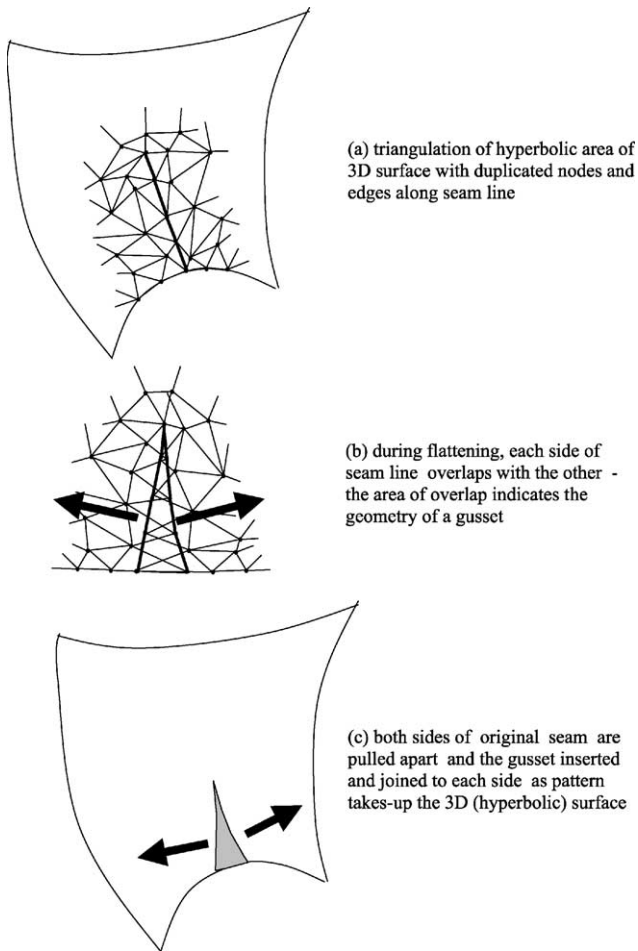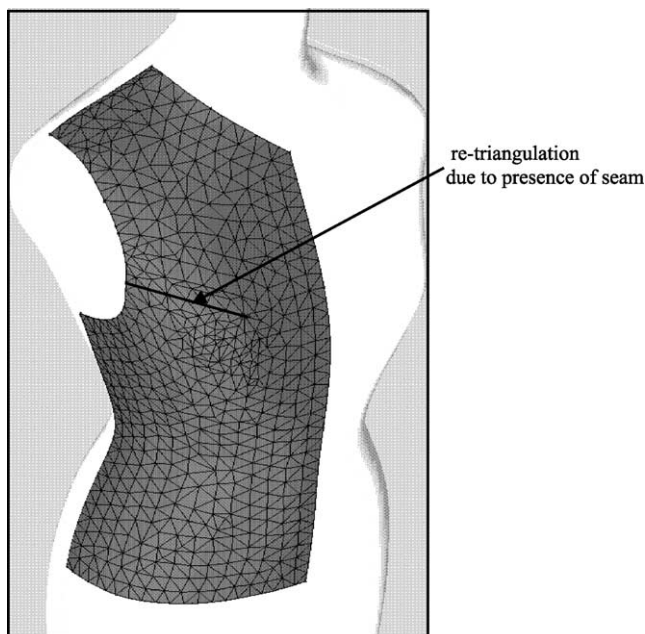
Fig. 6. Gusset formation in 2D pattern.

Fig. 7. Re-triangulation after seam insertion.

Thus, the energy model will calculate the strains implicit in distorting the 2D form of a triangle to its 3D representation.

Straining may vary over the 3D surface in that some triangles may have little or no in-plane strain while others may have significant amounts. In order to evaluate the energy required to apply this strain, the woven composition of a typical fabric is considered. Such fabrics commonly display different tensile behaviour in the warp and weft directions. For the purposes of this paper, linear tensile behaviour is assumed although more complicated non-linear models can easily be adopted. Hence, strain energy is assumed to originate from the fabric characteristics as expressed by K_{su} and K_{sv}, strain constants in the weft and warp directions, respectively (Fig. 8). Shear energy is similarly modelled by a shear strain constant K_r.

To analyse the distortion of the fabric, it is useful to concentrate on a single woven element. For such an element, the distortion that it undergoes when forcing the 2D pattern to take the 3D shape is assumed to be described by an affine transformation [14]. Fig. 9 details the three types of individual strains that contribute to the total distortion where u is the weft direction and v is the warp direction. It will be assumed that individual triangles will each have their own affine transformation to describe the distortion that the 2D triangle must undergo to take-up the equivalent 3D shape for the triangle. The flattening process will try different 2D geometric shapes for triangles in the 2D pattern. As a consequence, an energy value can be determined that is required to be applied to the 2D form in order for it to assume the 3D form. To calculate this associated energy for the triangle, it is necessary to superimpose the 2D and 3D shapes for the same triangle on a unifying warp and weft axes system. This requires that the warp and weft co-ordinate system must be superimposed on the 2D flattened (x, y) plane (Fig. 10). This structure is specified by the following parameters:

weft increment, w_{finc}
warp increment, w_{pinc}
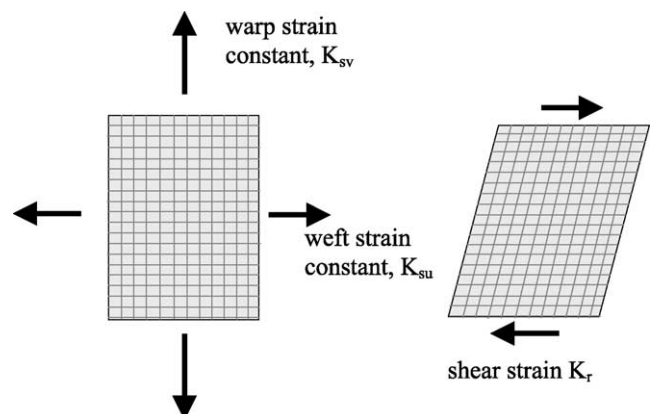grain direction, w_a.
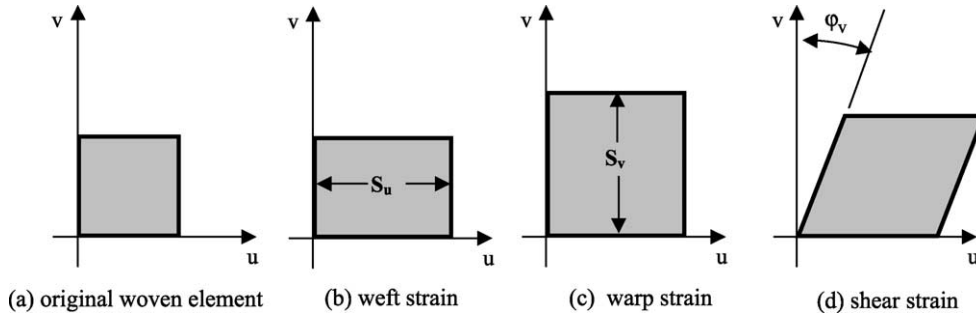

Fig. 8. Fabric strain constants.

Fig. 9. Affine transformations of woven element.

In effect, these parameters constitute a weft and warp axes system (w_f, w_p) for the pattern. Assuming that the (w_f, w_p) origin is located at the same position as the (x, y) origin, then a transformation can be used to provide (w_f, w_p) co-ordinates from (x, y) co-ordinates. Let the weft and warp increments in each of the directions w_f and w_p be represented by the vectors $\mathbf{w_f}$ and $\mathbf{w_p}$, respectively. These vectors will have magnitudes given by the w_{finc} and w_{pinc} values. Let w_a represent the grain direction defined as the angle that the weft direction makes with the x direction. Then these vectors can be defined as

$$\mathbf{w_f} = \begin{pmatrix} w_{finc}\cos(w_a) \\ w_{finc}\sin(w_a) \end{pmatrix} \tag{1}$$

$$\mathbf{w_p} = \begin{pmatrix} -w_{pinc}\sin(w_a) \\ w_{pinc}\cos(w_a) \end{pmatrix} \tag{2}$$

If a particular point on the (x, y) axes has co-ordinates (x_1, y_1), then these will be mapped to (w_{f1}, w_{p1}) on the weft and warp axes as follows:

$$w_{f1} = \mathbf{w_f} \cdot \begin{pmatrix} x_1 \\ y_1 \end{pmatrix} \tag{3}$$

$$w_{p1} = \mathbf{w_p} \cdot \begin{pmatrix} x_1 \\ y_1 \end{pmatrix} \tag{4}$$

Applying these formulae to each vertex of the triangle on the 2D (x, y) plane enables warp and weft co-ordinates to be calculated. This therefore enables both the 3D (A$'$, B$'$ and C$'$) and 2D (A, B and C) geometries for the same triangle to be unified on a (u, v) plane to provide the undistorted triangle shape and the strained 3D geometry for the triangle (Fig. 11). The convention adopted here is to locate one of the vertices (A and A$'$) at the origin for both 2D and 3D shapes. The 2D shape is then placed on (u, v) plane with the same orientation as for the 2D (x, y) flattening plane. The 3D triangle is then analysed to determine its orientation. However, by knowing the warp and weft co-ordinates for each vertex, it is possible to determine the particular orientation that has the weft direction aligned with the u axes. By superimposing these two triangles in this
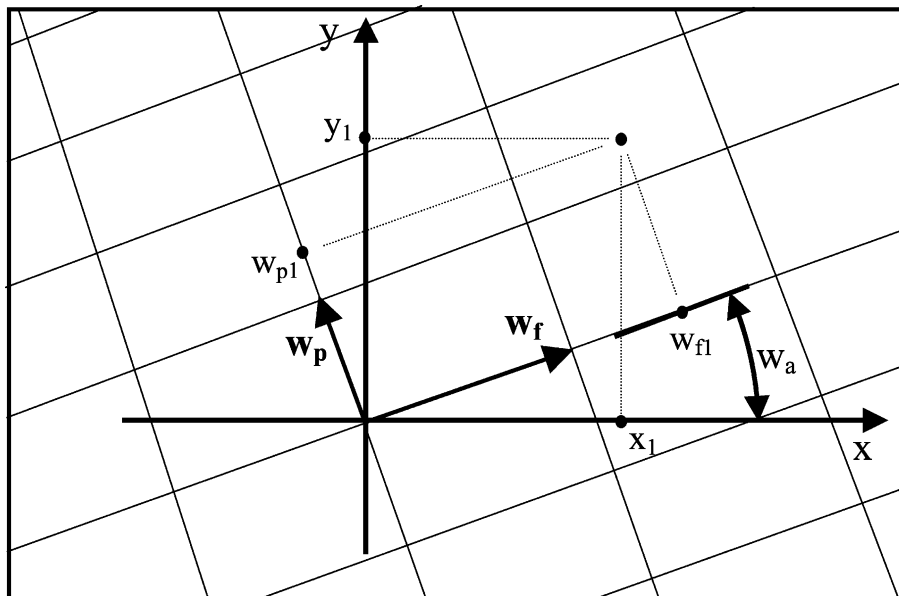
Fig. 10. Determination of warp and weft co-ordinates from (x, y) plane co-ordinates.
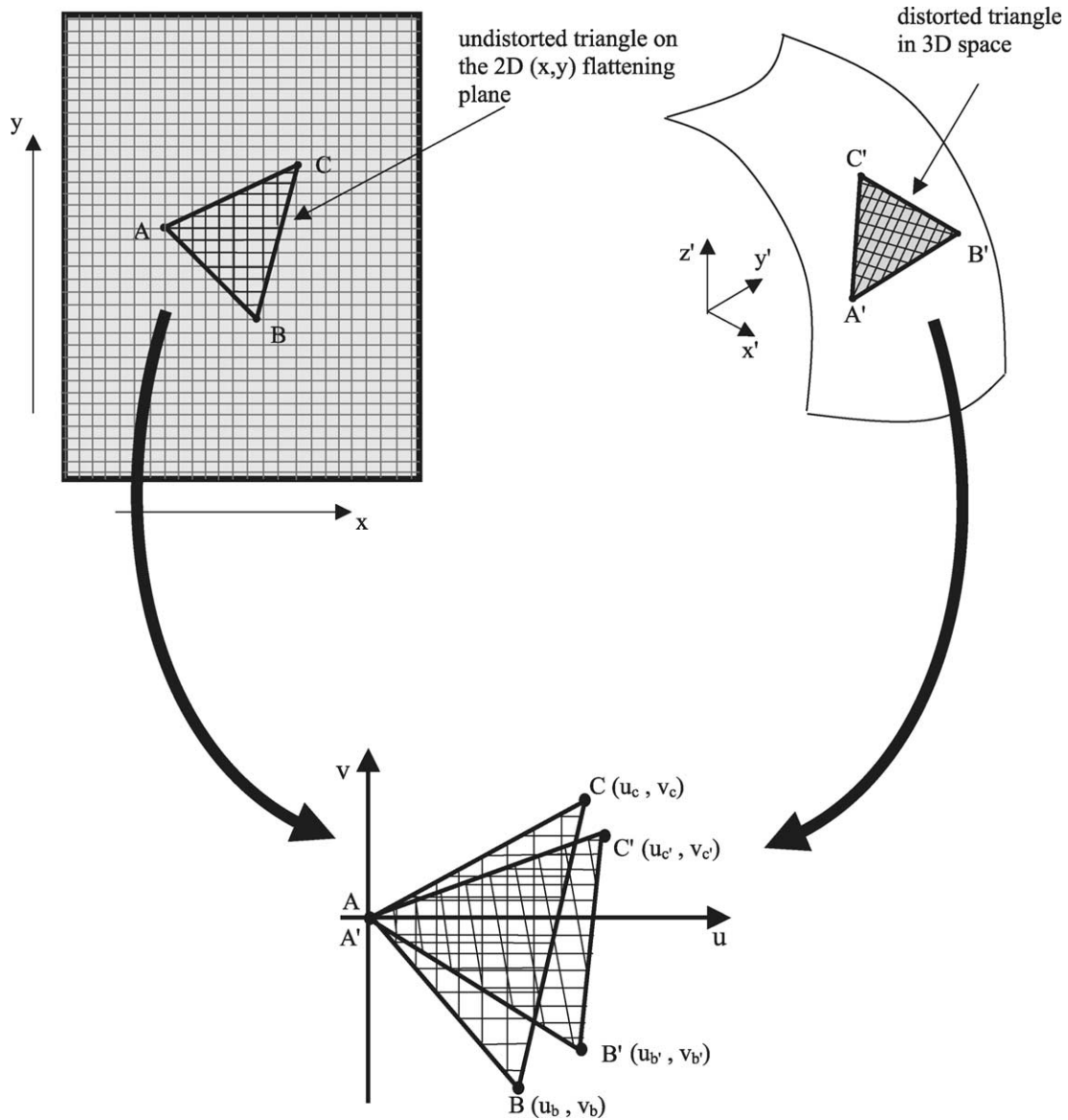
Fig. 11. Unified (u,v) plane for determining affine transformation for mapping 2D triangle shape to 3D triangle shape.

alignment, an affine transformation is in effect specified. Earlier work by the authors [15] has analysed the affine nature of this transformation and has derived equations to obtain the three strains S_u, S_v and φ_v from the locations for triangle vertices B, B$'$, C and C$'$.

These equations are

$$S_u = \frac{(v_C u_{B'} - v_B u_{C'})}{(u_B v_C - u_C v_B)} \tag{5}$$

$$\varphi_v = \tan^{-1}\frac{(u_B u_{C'} - u_C u_{B'})}{(u_B v_{C'} - u_C v_{B'})} \tag{6}$$

$$S_v = \frac{\sqrt{((u_B u_{C'} - u_C u_{B'})^2 + (u_B v_{C'} - u_C v_{B'})^2)}}{(u_B v_C - u_C v_B)} \tag{7}$$

Appendix A details the derivation of these equations.

Postle and Norton [16] have identified four modes to characterise fabric deformation of this type. These are fabric strain, fabric bending, in-plane yarn bending or shear and yarn twist. For this model, only the variation associated with strain and shear is considered. It is assumed that the energy associated with bending between triangles is a constant and is largely invariant when comparing different 2D patterns.

For the strain energy E_s associated with a single triangle

$$E_s = \iint (0.5\,K_{su}(S_u - 1)^2 \mathrm{d}u\,\mathrm{d}v + \iint (0.5 K_{sv}(S_v - 1)^2 \mathrm{d}u\,\mathrm{d}v$$

$$= 0.5A\{K_{su}(S_u - 1)^2 + K_{sv}(S_v - 1)^2\} \tag{8}$$

where A is the area of the 2D triangle and K_{su} and K_{sv} are the strain constants for the weft and warp directions, respectively.

The shear energy E_r, is given as

$$E_r = \iint (0.5 K_r \varphi_v^2) du\, dv = 0.5 A K_r \varphi_v^2 \qquad (9)$$

where K_r is the shear modulus.

Hence, given the point mappings described by Eqs. (5)–(7) above, the strain constants K_{su} and K_{sv} and the shear modulus K_r, the total strain energy $(E_s + E_r)$ required to deform the triangle can be calculated.

To summarise, the current energy of a partial or complete flattening is evaluated by following the procedure below for each triangle that has been flattened.

 (i) provide co-ordinates for each vertex in 3D (fixed)
 (ii) provide co-ordinates for each vertex in 2D (variable)
 (iii) unify both triangular forms on the the the (u,v) axes (Fig. 9) and so provide mappings for two vertices (Eq. (A.3))
 (iv) determine strains S_u, S_v and φ_v from point mappings by applying Eqs. (5)–(7)
 (v) use strain values and area of the 2D triangular form to determine the strain energy E_s and shear energy E_r using Eqs. (8) and (9).

6. Flattening process

The flattening process begins by attaching a medial distance to each triangle in the polygon list. This represents the shortest distance from the centre of area of each 3D triangle to the boundary of the panel. For the purposes of this calculation, a 3D seam line is treated as part of the boundary. This medial distance is then used to rank the polygons in a polygon list in the order of decreasing values of medial distance. Thus, the starting point for the flattening in 2D is to take the triangle that is furthest from the boundary (referred to here as a seed triangle) and to lay that

triangle arbitrarily down in 2D in a completely undistorted manner. This method is adopted because distortion tends to be cumulative when developing a 2D flattened pattern and forcing it to assume a 3D shape. Thus, if a flattening begins at some triangle on one side of the pattern, energy tends to build-up dramatically by the time the flattening reaches edges on the other side. The situation is obviously more complicated than this since the energy build-up is dependent on the curvature of the 3D surface. Once the first triangle has been laid down in 2D, the three neighbouring triangles can be flattened and so on. During this iterative process, if the 3D surface is not developable, it will soon emerge that a triangle must deform if it is to be flattened. The precise nature of the flattening algorithm is described elsewhere [8] which details how triangles can be flattened by either unconstrained or constrained flattening. Now follows a brief description of this algorithm.

Consider the flattening of a triangle T (Fig. 12). For unconstrained flattening, one edge $P_1 P_2$, of the triangle T has already been flattened while the third node P_3 has yet to be located on the flattening. The position of P_3 on the 2D flattening P'_3, is found by finding the intersection of two circles that does not lie within the boundary of the existing flattening to date. These circles are centred at P'_1 and P'_2 and have radii r_{13} and r_{23}, respectively, where r_{13} is the length of $P_1 P_3$ and r_{23} is the length of $P_2 P_3$ on the original 3D surface.

For constrained triangle flattening (Fig. 13), all three nodes (P'_1, P'_2 and P'_3) of a given triangle T' have been previously flattened although triangle T' itself has not yet been flattened. Assume now that triangle T' has a neighbour T_2 that has been previously flattened and provided an initial 2D position P'_3 for the 3D position P_3. However, when flattening T, P_3 is also the third node of T, which will possibly provide another location P'_3 on the 2D plane. This gives two 2D positions for point P_3. The conflict is resolved by analysing the energy states of the affected triangles
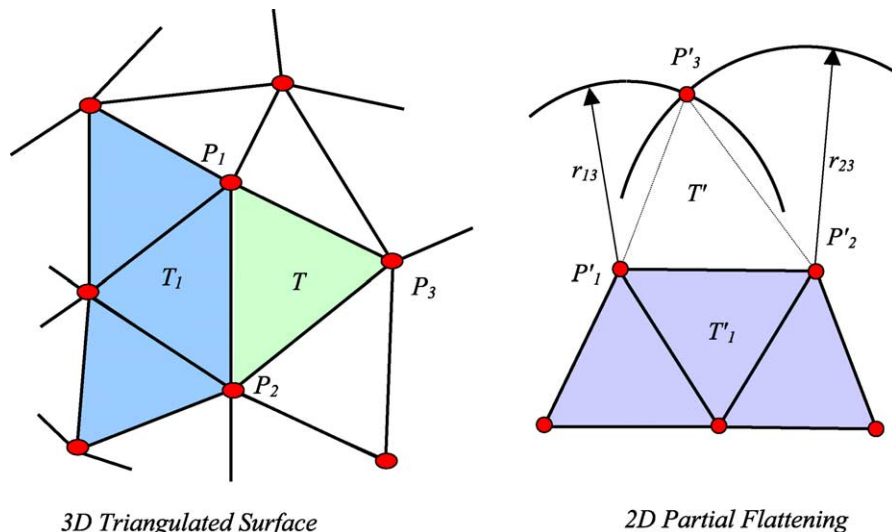

3D Triangulated Surface

2D Partial Flattening

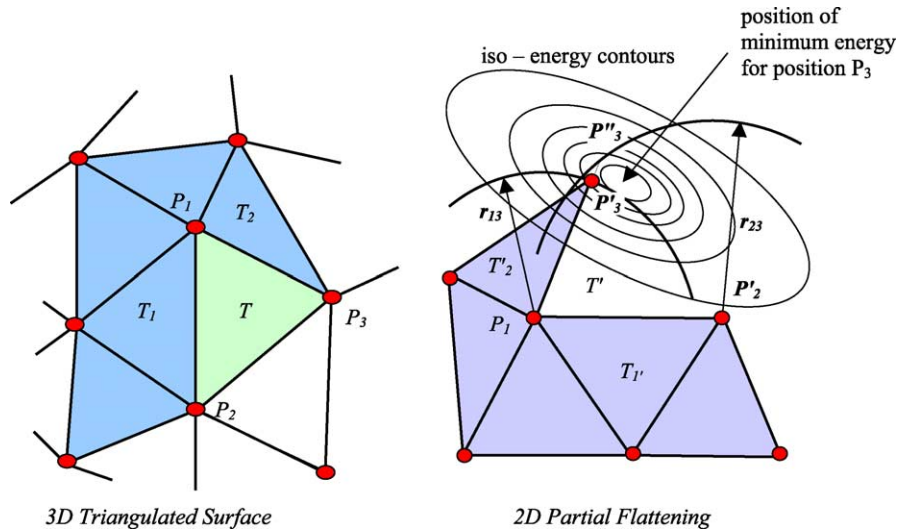Fig. 12. Unconstrained triangle flattening.

Fig. 13. Constrained triangle flattening.

(T and T_2). To visualise the local energy minimisation process that is applied, it is useful to consider superimposed energy contours as being present on the 2D plane when determining the best unique position for P_3 that yields minimum energy. A numerical gradient optimisation technique based on the Broyden–Fletcher–Goldfarb–Shanno method [17] has been incorporated into the algorithm whereby the 2D co-ordinates of P_3 are treated as variables. This search technique converges on the optimal 2D position for the node P_3.

Thus, the flattening process will also be able to provide a detailed energy map in terms of the three elemental strains. It will also be able to provide different flattenings depending on the orientation of the initial triangle with respect to the weave. Fig. 14 illustrates the progress of the flattening process as applied to the panel triangulation in Fig. 7. For this flattening the particular values of strain constants obtained by testing a sample fabric from industrial collaborators were:

$$K_{su} = 0.946 \text{ N/mm}, \quad K_{sv} = 0.548 \text{ N/mm},$$

$$K_r = 0.159 \text{ N/mm rad}.$$

7. Optimal seam siting

The flattening process described above provides a test platform for deciding the optimal configuration of a single seam in a particular garment panel. Seams that develop into darts or gussets should be considered as energy releasing mechanisms and if inserted into a panel can be expected to reduce the overall energy value for a particular 2D flattening. However, the positioning of seams should obviously be made in areas of large initial energy build-up so that their energy reducing capabilities are maximised. To illustrate this, consider the 14 possible sites for a seam in Fig. 15 for the same garment panel. When flattened with each of these seams, the energy levels of the 14 different flattenings will vary greatly. Considering Figs. 16 and 17, it can be seen that inserting a dart at seam s2 has little effect whereas inserting a dart at seam s8 results in the greatest energy reduction. Also, note the different flattenings produced by inserting seams at locations s8 compared to s11. Position s8 results in a dart construction whereas location s11 will require a gusset to be inserted at this
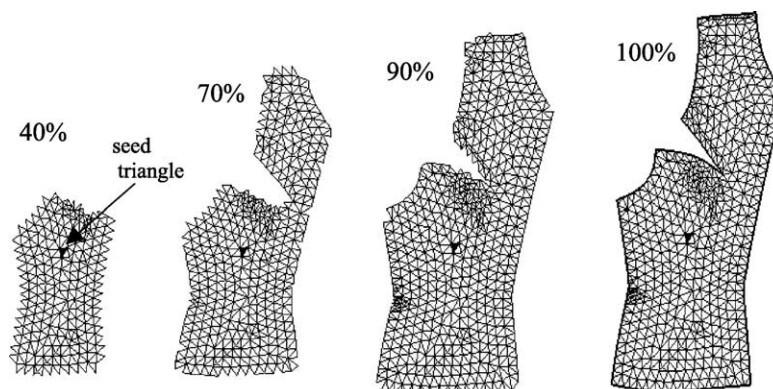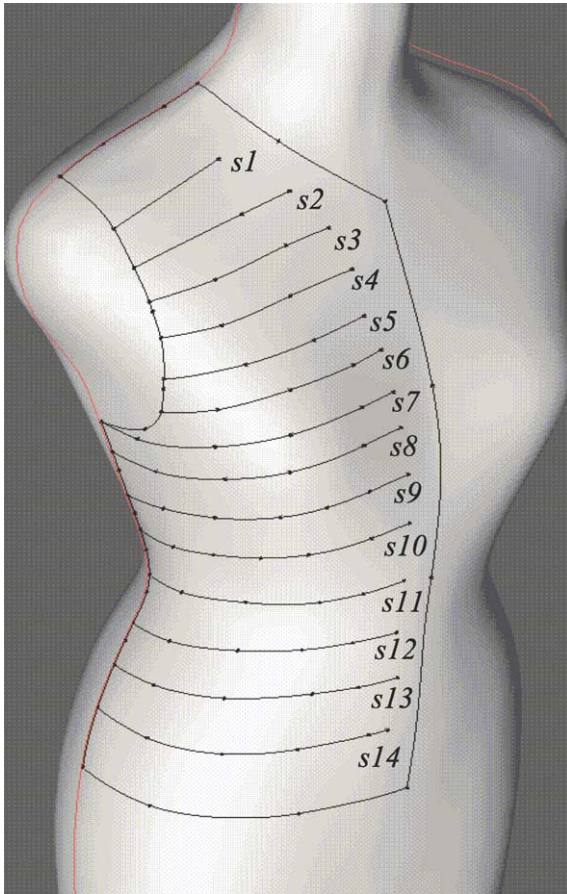

Fig. 14. Panel flattening progression.

Fig. 15. Location of test seams (s1–s14) on garment panel.

location. This is due to the fundamentally different types of curvature of the surface in the neighbourhood of each seam.

8. Sensitivity of flattening strains to fabric grain

Since the fabric model adopted is based on a woven structure, the strains that are inherent in the flattening are sensitive to the orientation of the pattern on the 2D plane. As indicated in Fig. 10, the grain direction sets the angle that the weft axis makes with the x axis on the 2D flattening plane. For garment manufacture where woven or knitted fabrics are used, the specification of a 2D pattern should in fact be relative to the grain direction. This will then unambiguously position the pattern on the fabric. Section 5 above, describes how the flattening process begins by arbitrarily locating a seed triangle on the 2D flattening plane. To be more precise, the angular orientation of this seed triangle on the 2D plane does influence the strain and energy distributions that ultimately result. It is thus necessary to indicate on the 3D triangulation in the area of the seed triangle, a preferred grain direction for the fabric. This angular relationship between the warp and weft directions and the 3D form of the seed triangle is then maintained during the initial positioning of the seed triangle on the 2D plane. Fig. 18 shows the three strain distributions that result by flattening the panel in Fig. 4 with no seam lines. As can be seen, the grain direction greatly influences the strain distributions in terms of the configuration and intensity. It is proposed that this kind of insight into how a particular pattern has to strain in order to take-up a 3D shape can assist in locating optimum grain direction. For instance, woven fabrics in general can strain more easily in shear. It would therefore be more advantageous to orientate the 2D pattern so that the direction of intense strain due to the underlying surface curvature is aligned with the shear direction. Conversely, the appearance of shear can be unsightly in some more noticeable areas of the garment concerned.

9. Discussion and conclusions

The work described here provides a means of flattening a 3D surface represented by a polygon mesh. It describes how a marching front technique has been used to provide
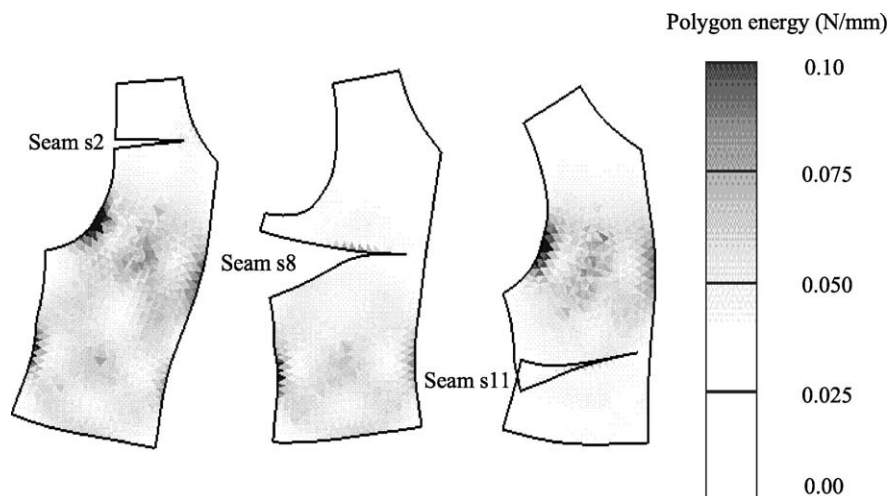

Fig. 16. Sample flattenings of garment panel with different seam locations.

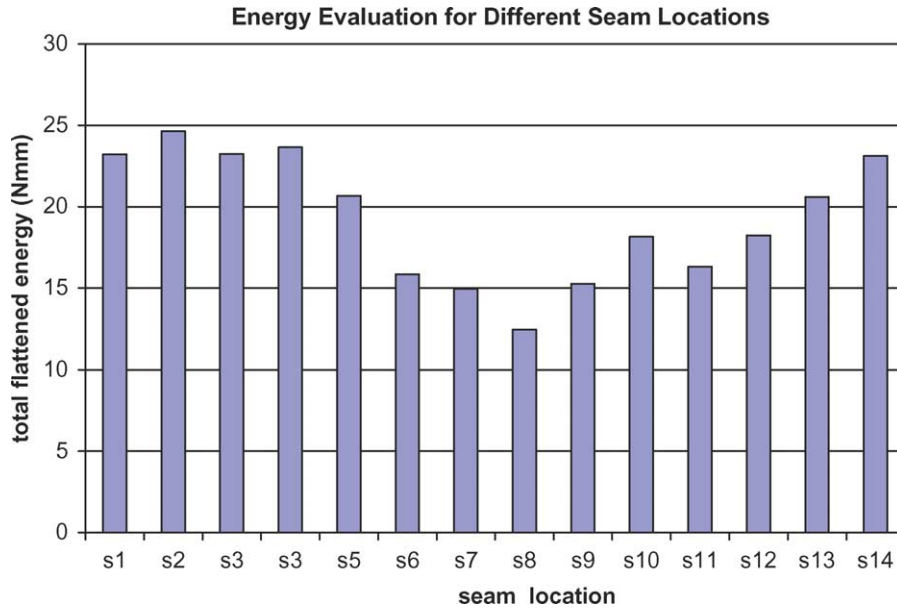**Energy Evaluation for Different Seam Locations**

Fig. 17. Energy variation due to different test seam locations.

triangulation that is sympathetic to the progress of the flattening algorithm. An energy model is proposed for quantifying the performance of a particular pattern when it is forced to assume a given 3D geometry. Also outlined is a process that reorganises the initial triangulation of the mesh if seams are to be used to improve the fitting process. The efficiency of a seam is quantified in terms of the reduction in the energy content implicit in the initial pattern. Although only single seams are illustrated, there is no reason why multiple seams cannot be used to greatly reduce the energy content of a given pattern. Although applied to a relatively simple panel here, the process described can be applied to any problem of this type with more complicated underlying body curvature. It is proposed that this method represents an objective method for both generating patterns with arbitrary seam configurations and evaluating the fitting performance in terms of an energy profile for a 2D pattern.

Work is continuing on this project and is currently concentrating on adaptive meshing whereby triangle intensification is automatically implemented for polygons found to contain comparatively large energy values during the flattening process.

Appendix A. Derivation of strain values from triangle distortion

The unified axes system outlined in Fig. 11 provides a means for comparing the change in shape of each triangle as it distorts from the zero energy 2D shape (ABC) to the 3D shape (A′B′C′). Since each triangle has a common position for the A and A′ vertex, the change in geometry resulting from the strains (S_v—1.0), (S_u—1.0) and φ_v is implicit in the change of locations from B to B′ and C to C′. Note that S_u and S_v are interpreted as scaling factors. The distortion of the triangle can be represented by an affine transformation [13]. The general representation of an affine transformation is

$$[\,u'\quad v'\quad 1\,] = [\,u\quad v\quad 1\,]\begin{pmatrix} a_{11} & a_{12} & 0 \\ a_{21} & a_{22} & 0 \\ a_{31} & a_{32} & 1 \end{pmatrix} \quad\quad (A.1)$$

For a particular affine transformation, the affine transformation matrix will now be referred to as $\mathbf{M}_{comp}$ where this matrix is comprised as follows

$$[\,u'\quad v'\quad 1\,] = [\,u\quad v\quad 1\,]\mathbf{M}_{comp}$$

and where

$$\mathbf{M}_{comp} = \begin{pmatrix} S_u & 0 & 0 \\ 0 & S_v & 0 \\ 0 & 0 & 1 \end{pmatrix}\begin{pmatrix} 1 & 0 & 0 \\ \sin\varphi_v & \cos\varphi_v & 0 \\ 0 & 0 & 1 \end{pmatrix}$$

$$= \begin{pmatrix} S_u & 0 & 0 \\ S_v\sin\varphi_v & S_v\cos\varphi_v & 0 \\ 0 & 0 & 1 \end{pmatrix} \quad\quad (A.2)$$

Note that this transformation represents collapsing shear as opposed to pure shear. For this type of shear, assuming S_u and S_v are both set to 1.0

$$u' = u + v\sin\varphi_v \quad\text{and}\quad v' = v\cos\varphi_v$$

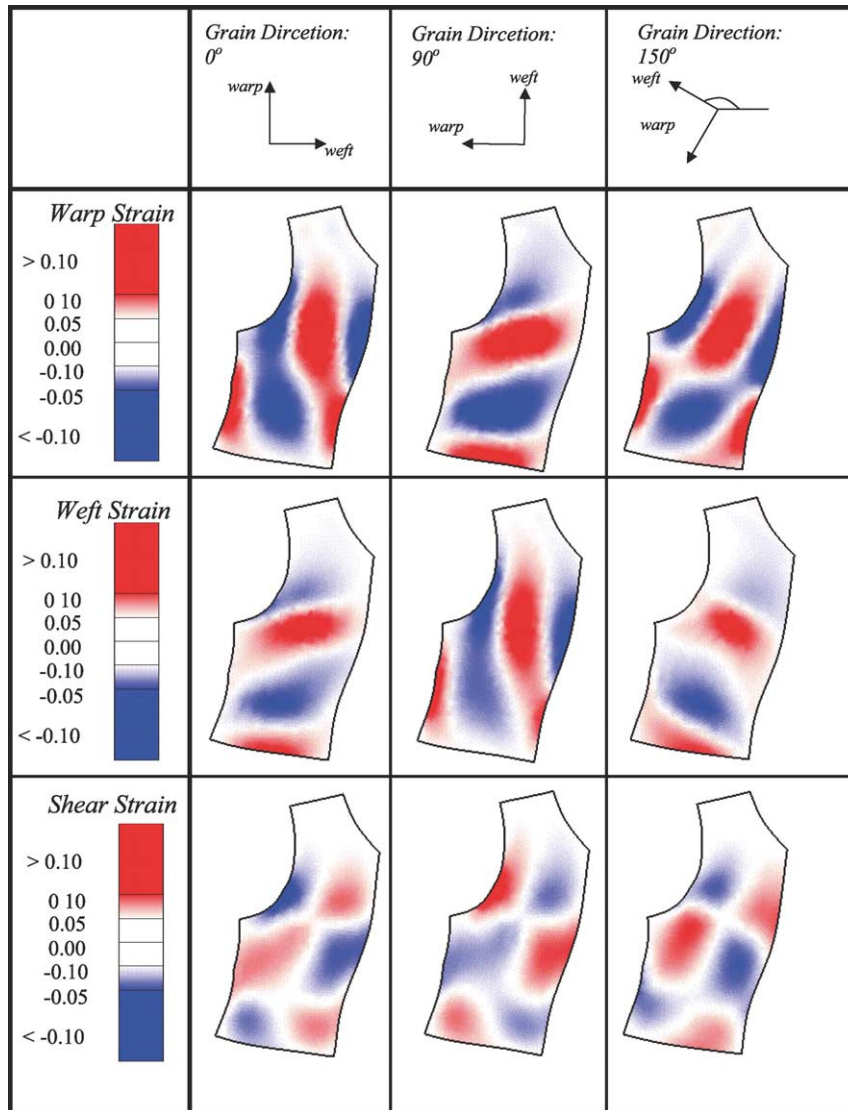The matrix in Eq. (A.2) is of affine form as described in Eq. (A.1).

Fig. 18. Sensitivity of warp, weft and shear strains to grain direction.

A particular affine transformation will be specified by the mapping of vertices B and C, i.e.

$$(u_B, v_B) \rightarrow (u_{B'}, v_{B'})$$
$$(u_C, v_C) \rightarrow (u_{C'}, v_{C'})$$

(A.3)

Eq. (A.1) can now be rewritten to include these two mappings and provide a means for solving for S_u, S_v and φ_v

$$\begin{pmatrix} 0 & 0 & 1 \\ u_{B'} & v_{B'} & 1 \\ u_{C'} & v_{C'} & 1 \end{pmatrix} = \begin{pmatrix} 0 & 0 & 1 \\ u_B & v_C & 1 \\ u_C & v_C & 1 \end{pmatrix} \begin{pmatrix} a_{11} & a_{12} & 0 \\ a_{21} & a_{22} & 0 \\ a_{31} & a_{32} & 1 \end{pmatrix}$$

or

$$\mathbf{U}' = \mathbf{U}\,\mathbf{A}$$

Hence

$$\mathbf{A} = \mathbf{U}^{-1}\mathbf{U}'$$

where

$$\mathbf{U}^{-1} = \frac{1}{\det(\mathbf{U})} \begin{pmatrix} (v_B - v_C) & v_C & -v_B \\ (u_C - u_B) & -u_C & u_B \\ (u_B v_C - u_C v_B) & 0 & 0 \end{pmatrix}$$

and

$$\det(\mathbf{U}) = (u_B v_C - u_C v_B)$$

This results in

$$\mathbf{A} = \frac{1}{\det(\mathbf{U})}$$

$$\times \begin{pmatrix} (v_C u_{B'} - v_B u_{C'}) & (v_C v_{B'} - v_B v_{C'}) & 0 \\ (u_B u_{C'} - u_C u_{B'}) & (u_C v_{B'} - u_C v_{B'}) & 0 \\ 0 & 0 & (u_B v_C - u_C v_B) \end{pmatrix}$$

(A.4)

By comparing Eqs. (A.2) and (A.4)

$$S_u = a_{11} = (v_C u_{B'} - v_B u_{C'})/(u_B v_C - u_C v_B) \qquad (A.5)$$

$$\varphi_v = \tan^{-1}(a_{21}/a_{22})$$

$$= \tan^{-1}((u_B u_{C'} - u_C u_{B'})/(u_B v_{C'} - u_C v_{B'})) \qquad (A.6)$$

$$S_v = \sqrt{(a_{21}^2 + a_{22}^2)}$$

$$= ((u_B u_{C'} - u_C u_{B'})^2 + (u_B v_{C'} - u_C v_{B'})^2)/(u_B v_C - u_C v_B) \qquad (A.7)$$

References

[1] Faux ID, Pratt MJ. Computational geometry for design and manufacture. Chichester: Ellis Harwood; 1985, p. 116.
[2] Manning JR. Computerised pattern cutting. Comput-Aided Des 1980;12:43–7.
[3] Hinds BK, McCartney J, Woods G. Pattern development for 3D surfaces. Comput-Aided Des 1991;23:583–92.
[4] Azariadis PN, Asparagathos NA. Design of planes developments of doubly curved surfaces. Comput-Aided Des 1997;29:675–85.
[5] Kim SM, Kang TJ. Garment pattern generation from body scan data. Comput-Aided Des 2003;35(7):611–8.
[6] Shaffer A, De Starler E. Smoothing an overlay grid to minimise linear distortion in texture mapping. ACM Trans Graphics 2002;21:874–90.
[7] Azariadis PN, Nearchon AC, Asparagathos NA. An evolutionary algorithm for generating planar developments of arbitrarily curved surfaces. Comput Ind 2002;47:357–68.
[8] McCartney J, Hinds BK, Seow BL. The flattening of triangulated surfaces incorporating darts and gussets. Comput-Aided Des 1999;31:249–60.
[9] Wang CL, Smith SF, Yuen MF. Surface flattening based on energy model. Comput-Aided Des 2002;34:823–33.
[10] Ohsaki M, Fujiwara J. Developability conditions for prestress optimisation of a curved surface. Comput Meth Appl Mech Eng 2003;192:77–94.
[11] Hinds BK, McCartney J, Hadden C, Diamond J. 3D Cad for garment design. Int J Clothing Sci Technol 1992;4(4).
[12] McCartney J, Hinds BK, Seow BL, Gong D. Dedicated 3D CAD for garment prototyping. J Mater Process Technol 2000;107(1–3):31–6.
[13] Lo HS. A new mesh generation scheme for arbitrary planar domain S. H. Lo. Int J Numer Meth Eng 1985;21:1403–26.
[14] Woolberg G. Digital image warping. Silver Spring, MD: IEEE Compter Society Press; 1990, p. 41–94.
[15] McCartney J, Hinds BK, Seow BL, Gong D. An energy base model for the flattening of woven fabrics. J Mater Process Technol 2000;107(1–3):312–8.
[16] Postle R, Norton AH. Mechanics of complex fabric deformation and drape. J Appl Polym Sci. Appl Polym Symp 1991;47:323–40.
[17] Vetterling WT, Teukolsky SA, Press WH, Flannery BP. Numerical recipes. 2nd ed. Example book [C]. Cambridge: Cambridge University Press; 1992 p. 168–84.

Jim McCartney holds the post of senior lecturer in the School of Mechanical and Manufacturing Engineering at the Queens University of Belfast. He has considerable experience in the development of 3D CAD systems for clothing and shoes. In particular he is interested in the processes of flattening 3D surfaces into 2D patterns and the reverse process of draping 2D patterns onto 3D templates. He has been involved in many government and industrial funded projects that have investigated these areas of research and is currently concentrating on the performance of materials during flattening and draping.

Brendan Hinds is currently a senior lecturer in the School of Mechanical and Manufacturing Engineering at the Queens University of Belfast. His academic interests include the modelling of fabric deformation, production process modelling, haptic modelling within the computer-aided design environment. He has participated in several collaborative research projects investigating the use of fabric drape modelling as a means of determining the fit and appearance of garments.

K.W. Chong after studying for his primary degree at TAR College in Malaysia, he gained a Master of Science degree in Manufacturing Systems with Distinction at Queen University, Belfast. He then carried out a research project investigating the flattening of triangulated surfaces and was awarded a PhD in 2002. His research interests include the development of marching front algorithms for triangulating bi-parametric surfaces and material energy minimisation during the flattening of 3D surfaces.